American Mineralogist, Volume 93, pages 886–892, 2008

Solubility of andradite, $Ca_3Fe_2Si_3O_{12}$, in a 10 mol% NaCl solution at 800 °C and 10 kbar: Implications for the metasomatic origin of grandite garnet in calc-silicate granulites

Jeremy L. Wykes,[1,2,*] Robert C. Newton,[2] and Craig E. Manning[2,†]

[1]Department of Earth and Marine Sciences, Australian National University, Canberra ACT 0200, Australia
[2]Department of Earth and Space Sciences, University of California at Los Angeles, Los Angeles, California 90095, U.S.A.

Abstract

The solubility of andradite garnet was determined at 800 °C and 10 kbar in a solution of 10 mol% NaCl and 90 mol% H_2O. Experiments were syntheses carried out with high-purity natural wollastonite, reagent hematite or natural specular hematite containing ~1 wt% TiO_2, and fluid. All experiments were performed with Mn_2O_3-Mn_3O_4 or Fe_2O_3-Fe_3O_4 oxygen buffers in a piston-cylinder apparatus with NaCl pressure media for 1–3 days. Andradite saturation was determined by the presence or absence of garnet in quenched charges.

Andradite dissolves incongruently to hematite and fluid with $CaSiO_3$ molality (m_{CS}) of 0.0838 ± 0.0015 for the reagent hematite and both buffers. Slightly higher m_{CS} of 0.0895 ± 0.0005 for the natural hematite and Mn-oxide f_{O_2} buffer is interpreted as due to incomplete equilibration and/or ~9 mol% Ti in the run-product andradite. Dissolved Fe molality could be determined only approximately, but must be at least ten times lower than m_{CS}. Quenched fluids were very basic (pH 11–12). The solubility of Fe_2O_3 in andradite-saturated H_2O-NaCl fluids is lower than that of Al_2O_3 at grossular saturation at the same pressure (P), temperature (T), and fluid composition.

The results permit a test of a model of $CaSiO_3$ dissolution in NaCl solutions to three dominant aqueous species: $CaCl^+$, OH^-, and H_3NaSiO_4. Combination of the $CaSiO_3$ molality at andradite saturation with wollastonite solubility at the same conditions (0.1253 ± 0.0047 molal; Newton and Manning 2006) leads to a Gibbs free energy change of the reaction 3 wollastonite + hematite = andradite at 800 °C and 10 kbar of –32.21 ± 2.45 kJ. The good agreement between this value and that derived from previous studies supports the dissolution model of $CaSiO_3$ in NaCl solutions. The low solubility of the Fe_2O_3 component of andradite contrasts with the high solubility of magnetite and of Fe in pelitic and granitic mineral assemblages measured in acidic chloride solutions by previous workers at lower P and T. The results imply that Fe_2O_3 is conserved during metasomatic processes affecting calc-silicates at high metamorphic grades.

Keywords: Experimental petrology, thermodynamics, fluid, crystal growth, metasomatism

Introduction

An important constituent of calc-silicate skarns and granulites is grandite garnet, a solid-solution dominated by andradite ($Ca_3Fe_2Si_3O_{12}$) and grossular ($Ca_3Al_2Si_3O_{12}$), with minor uvarovite ($Ca_3Cr_2Si_3O_{12}$). Grandite garnet-bearing assemblages have proven to be useful for determining the evolution of pressure (P), temperature (T), and fluid-rock interaction in skarns (Zhang and Saxena 1991) and calc-silicate assemblages in high-grade terranes (Sengupta et al. 1997; Sengupta and Raith 2002; Dasgupta and Pal 2005). However, identification of the processes by which andradite-rich garnet forms has been problematic. The skarn association is formed by metasomatic introduction of Fe and Si derived from igneous intrusions into carbonate wall rocks, often with deposition of important ores of Cu, W, Mo, and Fe (Burt 1972; Einaudi et al. 1981). Acidic, chloride-bearing magmatic fluids are implicated in this transport, as shown by the high solubility of magnetite (Chou and Eugster 1977; Boctor et al. 1980; Simon et al. 2004) and Fe in model pelitic and granitic compositions (Althaus and Johannes 1969; Whitney et al. 1985) measured at low pH (0–2) at 1–2 kbar and 300–700 °C. In contrast, Fe mobility appears to have been, for the most part, quite limited in high-grade gneisses, which has been interpreted to indicate virtual absence of mineralizing fluids (Buick et al. 1993). An evaluation of the cause of the apparent contrasts between these metamorphic environments would be possible if solubility data for andradite could be collected at granulite-facies conditions.

Most previous experimental studies of grandite garnet have been devoted to establishing the stabilities of the three end-members of the series, alone or in the presence of additional phases (Huckenholz 1969; Huckenholz and Yoder 1971; Gustafson 1974; Liou 1974; Huckenholz et al. 1974; Suwa et al. 1976; Taylor and Liou 1978; Moecher and Chou 1990), or their solid solutions (Huckenholz et al. 1974; Huckenholz and

* Present address: Clancy Exploration, 33 Leewood Drive, Orange, NSW 2800, Australia.
† E-mail: manning@ess.ucla.edu

0003-004X/08/0506–886$05.00/DOI: 10.2138/am.2008.2736

Knittel 1976). In contrast, there are few studies of the aqueous solubilities of the garnets at elevated *P* and *T*. Newton and Manning (2007) measured the solubility of grossular in NaCl-H_2O solutions at 800 °C and 10 kbar, in the NaCl mole fraction range 0–0.40. Grossular dissolves congruently at all salinities at these conditions. The measurements of Newton and Manning (2007) on synthetic grossular in pure H_2O are in good agreement with those of Fockenberg et al. (2004) on a natural grossular. The addition of NaCl causes a large enhancement of solubility. At $X_{NaCl} = 0.4$, the molality of $Ca_3Al_2Si_3O_{12}$ is 26× higher than in pure H_2O at the same conditions. The most significant enhancement effect is the high solubility of Al_2O_3, a component long regarded as inert in fluid-rock metamorphic processes (e.g., Carmichael 1969). Although corundum possesses relatively low solubility in pure H_2O at similar conditions (Tropper and Manning 2007), its solubility can be enhanced by complexing with Si (Manning 2007). However, in solutions containing both NaCl and $CaSiO_3$, Al_2O_3 molality can be at least 130× as great at 800 °C and 10 kbar as in pure H_2O at the same conditions (Newton and Manning 2007). In contrast, the solubility of wollastonite ($CaSiO_3$), although greatly enhanced by NaCl at high *T* and *P* (Newton and Manning 2006), is only slightly higher in the presence of Al_2O_3. This finding implies that the driving force for grossular and corundum solubility enhancement in the system $CaSiO_3$-Al_2O_3-NaCl-H_2O is the stability of Ca chloride and more-extensive formation of Na-Al ± Si complexes relative to Ca-Al ± Si complexes. Further insight is gained from results of Newton and Manning (2006), which showed that solubilities, expressed as mole fractions of corundum and wollastonite, increase with increasing NaCl to well-defined maxima at X_{NaCl} = 0.14 and 0.33, respectively. This finding strongly indicates that the solute products are hydrous, and that destabilization of the solute hydrates with decreasing H_2O activity eventually overcomes the initial enhancement effect of NaCl on Al_2O_3 and $CaSiO_3$, causing solubility to decline with further NaCl increase. The same effect of destabilization of hydrous complexes with increasing NaCl is apparent in grossular solubility, as with its components Al_2O_3 and $CaSiO_3$, although the data of Newton and Manning (2007) do not define a clear maximum.

The present work expands the scope of garnet solubility data by comparing the dissolution behavior of andradite with that of grossular at 800 °C, 10 kbar, and $X_{NaCl} = 0.1$. We investigated whether andradite is, like grossular, congruently soluble and whether the solubility of Fe^{3+} is enhanced in a manner similar to that of Al. The results provide an independent test of the model of Newton and Manning (2006) for $CaSiO_3$ dissolution in NaCl solutions and offer insights into Fe^{3+} mobility in metamorphic systems.

Experimental methods

The experiments were carried out in a piston-cylinder apparatus with NaCl pressure medium and graphite heater sleeves. Both 1 in. (2.54 cm) and ¾ in. (1.91 cm) diameter pressure chambers were used. Methods of Newton and Manning (2006) and Tropper and Manning (2007) were employed. Temperatures, measured and controlled automatically with Pt-$Pt_{90}Rh_{10}$ and $W_{97}Re_3$-$W_{75}Re_{25}$ thermocouples, are considered accurate to ±3 °C. Pressures, measured by Heise Bourdon tube gauges, are accurate to ±0.2 kbar.

Starting materials were natural hematite, synthetic reagent hematite, and natural high-purity wollastonite. Cleavage fragments of natural hematite were taken from a large crystal of specular hematite, cut to the desired size, rolled in SiC paper, ultrasonically cleaned in distilled water, and then held at 600 °C overnight (Fig. 1). Analyses by energy dispersive spectroscopy (Table 1) show that it contains 0.89 wt% TiO_2 as the only significant impurity. Synthetic, reagent-grade hematite (Baker, 99.9% purity) was heated at 600 °C for 5 days in a platinum crucible, pressed into a pellet, and then sintered at 700 °C for 48 h. Fragments from the sintered pellet were then ground, cleaned, and heated as above (Fig. 1). X-ray diffraction (XRD) confirmed that the treatment yielded pure hematite. The wollastonite was the same material used by Newton and Manning (2006).

An attempt was made to prepare synthetic andradite suitable for solubility measurements. About 50 mg of a fine-grained mixture of the natural wollastonite and reagent hematite were sealed with ~20 mg of H_2O by arc welding in an Au tube segment. The charge was held at 850 °C and 10 kbar for 36 h, with a yield of ~29 mg of very fine-grained andradite. The cubic unit cell constant was determined by XRD scans (1/2 °2θ, Cu*K*α radiation) to be 1.2054 ± 0.0011 nm, identical to the OH-free andradite end-member of Gustafson (1974). However, the andradite contained hematite inclusions and was not usable as a starting material.

Experimental charges were prepared by placing a single crystal of wollastonite as a $CaSiO_3$ source with one or several chips of hematite, together with ~12 ± 2 mg NaCl, in 3.5 mm O.D. Platinum or gold tube segments. The hematite grains were in some cases encapsulated in a crimped and/or pierced inner platinum capsule (1.5 mm O.D.; Fig. 1); however, this step proved unnecessary, and was abandoned. An NaCl mole fraction of 0.1 was obtained by adding a slight excess of H_2O via syringe and then allowing evaporation to the mass required given the NaCl weight. Once the desired fluid composition was attained, the weight of H_2O (H_2O in) was recorded and capsules were crimped and sealed by arc welding (Fig. 1).

It was necessary to control oxygen fugacity (f_{O_2}) at a relatively high level to avoid synthesis of Fe^{2+} phases such as hedenbergite. Buffering was accomplished in two ways. In some experiments, a capsule was added that contained a mix of 80 wt% fine-grained bixbyite, Mn_2O_3, and 20 wt% hausmannite, Mn_3O_4 (prepared from reagent MnO_2 by firing at 800 °C for ≥18 h). Ten milligrams of the bixbyite-hausmannite (BH) buffer mix was sealed with 2 mg H_2O in a 1.6 mm O.D. Platinum tube with wall thickness 0.1 mm. At equilibrium, the BH buffer fixes f_{O_2} at ~6 log units higher than the hematite-magnetite (HM) equilibrium. In other experiments, an overwhelming amount of reagent-grade hematite was added with the wollastonite. Hematite partially reacted to magnetite during all such experiments, to give f_{O_2} of the HM buffer. It was found that more than ~10 mg of hematite were required to ensure incomplete conversion to magnetite; only runs in which both buffer minerals were present at the end of an experiment have been included in the data set.

Table 1. Energy-dispersive analysis of natural specular hematite

Si	0.07(05)
Ti	0.89(21)
Al	0.05(05)
Fe	68.56(66)
O	30.25(40)
Total	99.82(55)

Note: Entries, in wt%, are average of 10 analyses, with 1σ uncertainty in last digits.

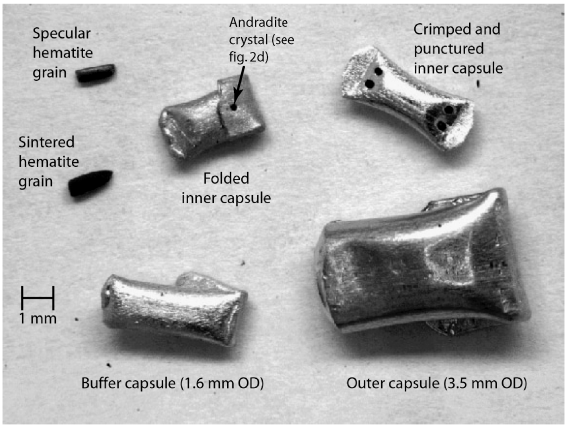

Figure 1. Components of the experimental capsules for experiments, including hematite chip and pellet, inner capsules for hematite, inner f_{O_2} buffer capsule containing Mn oxides plus H_2O, and loaded and folded outer capsule.

In BH-buffered runs, no magnetite formed in the hematite chip of 1–3 mg mass: the buffer was apparently completely effective in holding the oxygen fugacity in the hematite field. XRD scans of the quenched buffer material showed that both Mn oxides were still present.

The pH of the quenched fluid from one experiment was determined by placing a strip of pH paper in contact with the fluid as it oozed out of the capsule after puncturing with a needle. In this experiment, it was impossible to measure the H_2O after the experiment by drying weight loss. In a few other experiments, the fluid sprayed out forcefully when the capsule was punctured, which compromised the measurement of H_2O after quench (H_2O out). In most other experiments, the weight of H_2O as determined by drying loss matched the weight of the H_2O initially weighed into the capsule to within 0.6% relative.

Weights of H_2O and NaCl were determied using a Mettler M3 microbalance ($1\sigma = 3$ µg). Hematite and wollastonite were weighed on a Mettler UMX2 ultramicrobalance ($1\sigma = 0.25$ µg). Complete dissolution of wollastonite allows m_{CS} to be calculated from the weight of loaded wollastonite; in several cases, hematite chips could be weighed after the run, permitting determination of Fe molality (m_{Fe}) from the weight loss. Propagation of these errors to fluid compositions yield 1σ uncertainties in X_{NaCl}, m_{CS}, and m_{Fe} of 3×10^{-5}, 1×10^{-4}, and 1×10^{-5}, respectively.

Experimental results

Textures of quenched charges

Run products were characterized by optical microscopy and, in selected cases, by scanning-electron microscopy. No evidence for residual, undissolved wollastonite was observed in the quenched charges. The reagent-grade hematite was coarsely recrystallized to flat hexagonal crystals (Fig. 2a) interspersed in HM-buffered runs with magnetite octahedra (Fig. 2b). Thin tapered blades of quench wollastonite were encountered in all experiments (Fig. 2b), as in previous work (Newton and Manning 2006).

Andradite was identified by optical and scanning-electron microscopy. The crystals had characteristic dodecahedral crystal faces and in grain mounts were isotropic, with a refractive index much greater than 1.7. Two textural types were observed. The first was large (20–50 µm in diameter), limpid, light-yellow equant crystals. These crystals chiefly occur either on the surfaces of hematite chips (Fig. 2c) or on the surfaces of inner capsules (Figs. 1 and 2d). A second form of andradite was tiny (<5 µm) dodecahedra scattered throughout runs with natural hematite (Fig. 2e). The uniformity of size and distribution of these crystals, and their restriction to natural-hematite runs, indicates that they were formed during quench. The texture of the tiny andradite crystals is strikingly similar to the quench-calcite rhombs described by Caciagli and Manning (2003).

The remaining products after quenching and drying were masses of skeletal halite and the flocculated masses of tiny white spheres, or "fish roe" (Fig. 2f). Both are typical of high *P-T* solubility studies involving silicate minerals (e.g., Newton and Manning 2006, 2007).

Solubility constraints

Experiments with natural specular hematite. Results of the experiments are given in Table 2 and Figure 3. The threshold m_{CS} for the appearance of andradite was found to be between 0.0892 and 0.0897 for experiments with the natural specular hematite and the BH f_{O_2} buffer. The andradite contained about 4 wt% TiO_2 (Table 3), which corresponds to 91 mol% $Ca_3Fe_2Si_3O_{12}$ and 9 mol% $Ca_3Fe_2Ti_3O_{12}$ (Ti-andradite), assuming that all Ti replaces Si (Huckenholz 1969).

Quantitative characterization of the molality of Fe was attempted in early experiments using natural hematite, but proved to be difficult. The natural hematite chips were quite coherent, and could be retrieved intact from quenched charges; however, they were coated with quench products and had to be cleaned ultrasonically, which could have resulted in slight mass losses. The four experiments in which a determination could be made limit m_{Fe} to between 0.0079 and 0.0140 (Table 2), and suggest a weak positive correlation with m_{CS} (the highest m_{Fe} value neglects the small amount of andradite intergrown with hematite). Possible loss of material during cleaning renders the concentrations maximum values only. Regardless, the data show that, in a solution of $X_{NaCl} = 0.1$, the ratio m_{CS}/m_{Fe} is at least 8 ± 1. Because congruent dissolution of andradite would yield molar $m_{CS}/m_{Fe} = 1.5$, the experiments with natural specular hematite show that andradite dissolution is strongly incongruent at the conditions of this study.

Experiments with reagent-grade Fe_2O_3. Andradite ap-

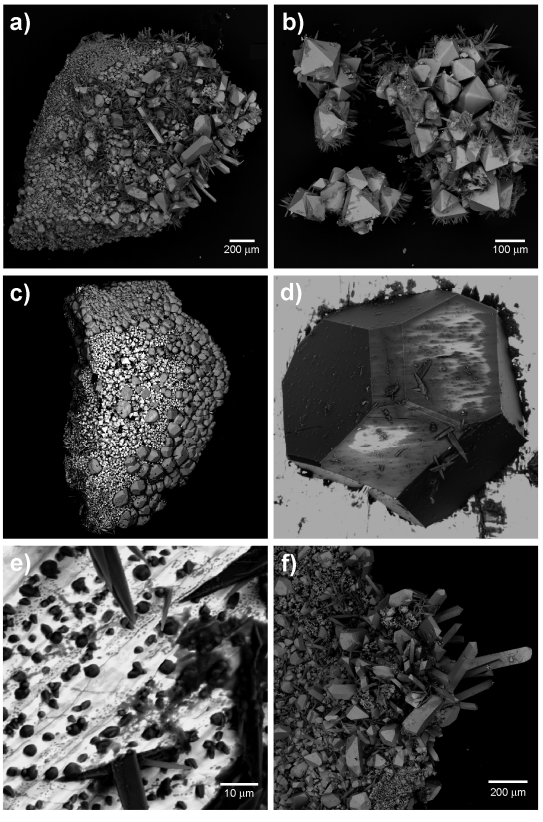

Figure 2. Secondary electron images of portions of quenched charges. (**a**) Surface of recrystallized sintered pellet of reagent hematite showing coarse-grained hematite, Run JW-74 (Table 3). (**b**) Magnetite octahedra and bladed, quench wollastonite, Run JW-74. (**c**) Andradite formed by reaction of reagent hematite and solute $CaSiO_{3,aq}$, Run JW-72. Aggregate is ~1.5 mm in long dimmension. (**d**) Large andradite perched on inner capsule wall. Crystal is ~0.25 mm across. (**e**) Andradite crystals on outer capsule wall (background), interpreted to have grown during quench, with blades of quench wollastonite, Run JW-31. (**f**) Recrystallized hematite pellet with minute siliceous spheres ("fish roe") in interstices between crystals, Run JW-74.

TABLE 2. Experimental results

Exp. no.	Hematite and capsule types	f_{O_2} buffer	Time (h)	NaCl in (mg)	H_2O in (mg)	H_2O out (mg)	X_{NaCl}	Hm in (mg)	Hm out (mg)	$CaSiO_3$ in (mg)	m_{CS}	m_{Fe}	Stable assemblage and notes
JW-27	N/Pt	BH	18	9.801	27.078	n.d.	0.100	1.3413	n.d.	0.1851	0.0588		Hm
JW-30	N/Pt	BH	18	8.669	24.510	24.522	0.098	1.1165	1.1010	0.2015	0.0708	0.0079	Hm
JW-31	N/Pt	BH	19	8.692	24.281	24.272	0.099	1.1994	1.1798	0.2244	0.0796	0.0101	Hm
JW-35	N/Pt	BH	16	9.155	27.732	n.d.	0.092	2.1866	n.d.	0.2731	0.0848		Hm
JW-34	N/Pt	BH	21	10.55	29.233	29.252	0.100	0.8024	n.d.	0.2880	0.0848		Hm
JW-36	N/Pt	BH	16	10.065	28.026	28.039	0.100	0.6531	0.6321	0.2895	0.0889	0.0094	Hm
JW-32	N/Pt	BH	23	10.272	28.382	n.d.	0.100	1.2276	n.d.	0.2966	0.0900		Hm,Ad
JW-29	N/Pt	BH	20	9.355	25.597	n.d.	0.101	0.7606	0.7319	0.3075	0.1034	0.0140	Hm,Ad
JW-78	R/Au	HM	45	12.851	35.629	35.861	0.100	48.960	n.d.	0.3235	0.0782		Hm,Mt
JW-80	R/Au	HM	74	9.256	25.671	n.d.	0.100	37.578	n.d.	0.2454	0.0823		Hm, Mt*
JW-77	R/Pt	HM	50	14.003	38.541	39.203	0.101	24.3660	n.d.	0.3839	0.0857		Hm,Mt,Ad
JW-79	R/Au	HM	20	13.239	36.704	36.880	0.100	42.506	n.d.	0.3652	0.0857		Hm,Mt,Ad
JW-76	R/Pt	HM	50	12.539	34.764	34.857	0.100	23.0290	n.d.	0.3594	0.0890		Hm,Mt,Ad
JW-74	R/Pt	HM	29	11.830	32.738	32.870	0.100	36.6949	n.d.	0.3423	0.0900		Hm,Mt,Ad
JW-73	R/Pt	HM	48	13.359	37.176	34.531	0.100	6.7862	n.d.	0.4275	0.0990		Hm,Mt,Ad
JW-72	R/Pt	HM	16	13.392	36.934	36.943	0.100	4.3320	n.d.	0.9322	0.2173		Hm,Mt,Ad
JW-82	R/Au	BH	70	10.978	30.446	30.412	0.100	2.6280	n.d.	0.2915	0.0824		Hm
JW-81	R/Au	BH	62	10.269	28.474	n.d.	0.100	3.0303	n.d.	0.2812	0.0850		Hm,Ad

Notes: Abbreviations: CS = $CaSiO_3$; n.d. = not determined; N = natural hematite; R = synthetic reagent hematite; Pt = Pt outer capsule; Au = Au outer capsule; BH = bixbyite-hausmannite f_{O_2} buffer; HM = hematite-magnetite f_{O_2} buffer; Hm = hematite; Mt = magnetite; Ad = andradite. Propagation of weighing errors of 3 µg (H_2O and NaCl) and 0.25 µg (wollastonite and hematite) yields uncertainties in X_{NaCl}, m_{CS}, and m_{Fe} of 3×10^{-5}, 1×10^{-4}, and 1×10^{-5} (see text).
* Quench pH = 11–12.

TABLE 3. Wavelength dispersive analysis of andradite from natural-hematite experiments

	Weight percent oxides				Cations/16 cations		
	Average	Minimum	Maximum		Average	Minimum	Maximum
SiO_2	31.26	30.65	31.93	Si	5.45	5.37	5.51
TiO_2	4.39	3.89	4.99	Ti	0.58	0.5	0.65
Al_2O_3	0.03	0.02	0.04	Al	0.00	0.00	0.00
Cr_2O_3	0.02	0.00	0.04	Cr	0.00	0.00	0.00
Fe_2O_3*	29.61	29.34	30.18	Fe	3.89	3.87	3.92
MnO	0.03	0.01	0.07	Mn	0.00	0.00	0.01
MgO	0.13	0.10	0.17	Mg	0.04	0.03	0.04
CaO	32.52	32.34	32.7	Ca	6.07	6.04	6.14
Na_2O	0.07	0.04	0.10	Na	0.02	0.01	0.03
K_2O	0.00	0.00	0.00	K	0.00	0.00	0.00
Totals	98.06	96.39	100.22		16.05	15.82	16.30

* All Fe as Fe_2O_3.

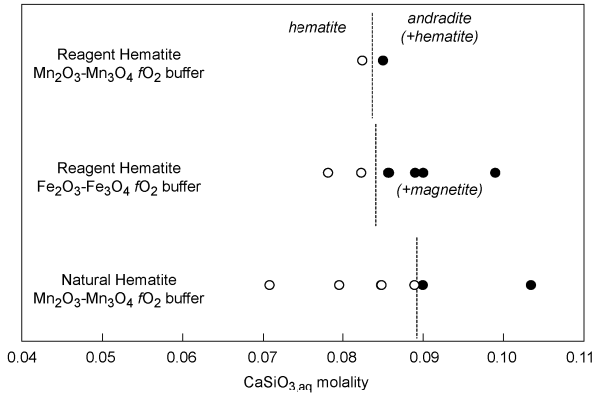

FIGURE 3. Results of synthesis runs on hematite and $CaSiO_3$ with different starting hematite and different f_{O_2} buffers. All experiments at 800 °C, 10 kbar, and in the presence of a fluid of composition 90 mol% H_2O, 10 mol% NaCl (neglecting dissolution products). Filled symbols represent synthesis of garnet and are plotted as apparent $CaSiO_{3,aq}$ molality calculated assuming all $CaSiO_3$ was dissolved in the fluid phase. Open symbols represent hematite ± magnetite only in run products; actual $CaSiO_{3,aq}$ concentrations are obtained in these experiments. The $CaSiO_{3,aq}$ concentration in the presence of hematite and garnet is invariant at a composition between filled and open symbols; dashed lines show the midpoint compositions, which are used in the text.

peared between m_{CS} of 0.0823 and 0.0856 for the experiments with reagent-grade hematite, independent of f_{O_2} buffer (Fig. 3). The recovered chips of hematite were coarsely recrystallized on the surfaces, and somewhat friable. In one case (JW-82), it was possible to transfer the hematite quantitatively into a weighing pan, but adhering quench precipitate could not be removed ultrasonically, which prevented accurate weighing. The pH of the quenched fluid from experiment JW-80 was 11–12, as is typical for all solubility measurements in NaCl solutions involving $CaSiO_3$ (Newton and Manning 2006).

Equilibrium considerations. These experiments are syntheses of andradite from less stable starting materials and thus strictly provide only upper limits to the equilibrium solubility. However, the reproducibility in runs using reagent-grade hematite that differ in duration by a factor of about two (JW-77 and JW-79, Table 2) suggest that equilibrium was attained. In addition, the presence in some charges of myriad tiny quench andradite crystals suggests a low energetic barrier to andradite nucleation, in contrast to the inhibited nucleation exhibited in experimental studies of other garnets.

DISCUSSION

On the basis of our measurements and observations, we conclude that, at 800 °C and 10 kbar in the presence of a solution of 10 mol% NaCl, andradite dissolves incongruently, leaving a residue

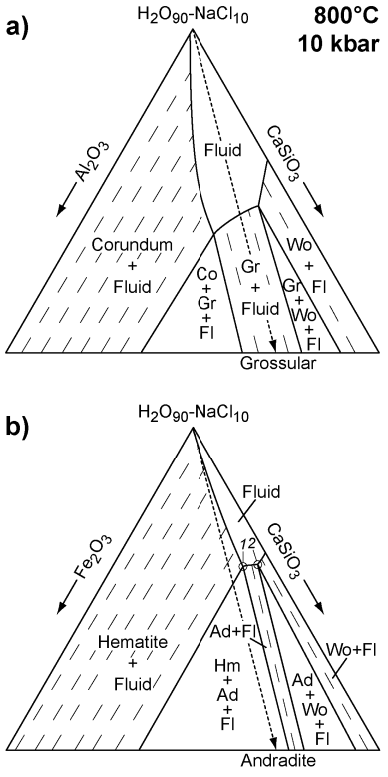

FIGURE 4. Schematic phase relations among garnet, wollastonite, oxide minerals, and a fluid of composition 90 mol% H_2O, 10 mol% NaCl in the systems fluid-Al_2O_3-$CaSiO_3$ (**a**) and fluid-Fe_2O_3-$CaSiO_3$ (**b**). Abbreviations: Ad = andradite; Co = corundum; Fl = fluid; Gr = grossular; Hm = hematite; Wo = wollastonite. Fluid is present in all fields. Dotted lines are the joins garnet-fluid. The major difference in the diagrams is the incongruent solubility of andradite (**b**) as contrasted with the congruent solubility of grossular (**a**). Point 1 in **b** gives the composition of the isothermal, isobaric invariant fluid in equilibrium with andradite and hematite, and point 2 is the fluid composition in equilibrium with andradite and wollastonite.

of hematite. Dissolved Fe is about ten times lower than dissolved $CaSiO_3$, on a molar basis. Equilibrium $CaSiO_3$ molality is 0.0838 ± 0.0015 in experiments with reagent-grade hematite. Slightly higher m_{CS} of 0.0895 ± 0.0005 observed for Ti-bearing andradite formed from natural hematite may reflect incomplete equilibration. It is not clear why the small 9% replacement of Si by Ti in the garnet should result in a somewhat higher solubility value from that yielded by the reagent-grade hematite experiments. It is noteworthy that the experiment that constrains andradite undersaturation (JW-36) was only 16 h in duration. It is possible that andradite nucleation was kinetically impeded near the saturation boundary due to a very low free energy overstep. Due to the Ti impurity and possible incomplete equilibration, we use the solubility determined from reagent-grade Fe_2O_3 for all calculations below.

Phase-equilibrium implications

Figure 4 shows schematic plots of the phase relations of grossular in the system $CaSiO_3$-Al_2O_3-NaCl-H_2O and andradite in the system $CaSiO_3$-Fe_2O_3-NaCl-H_2O at 800 °C, 10 kbar, and constant (moderate) salinity. The major difference between the two systems is the congruent dissolution of grossular as opposed to the incongruent dissolution of andradite. This occurs because of the much lower solubility of hematite than of corundum in $CaSiO_3$-H_2O-NaCl fluids. As a consequence, andradite-saturated compositions along the join $Ca_3Fe_2Si_3O_{12}$-H_2O (at constant salinity) must coexist with hematite and a fluid at invariant point 1 (Fig. 4). A fluid stable with only andradite must have a composition more $CaSiO_3$-rich than the join (H_2O_{90}-$NaCl_{10}$)-$Ca_3Fe_2Si_3O_{12}$. For bulk compositions still richer in $CaSiO_3$, andradite + wollastonite coexist with a fluid of composition 2 (Fig. 4). The $CaSiO_3$ molality at this point would be expected to be negligibly different from the value at the same T, P, and salinity measured by Newton and Manning (2006), because of the very small solubility of hematite. This circumstance makes possible a theoretical analysis of the solubility of andradite at the present experimental conditions.

Newton and Manning (2006) inferred that the dominant dissolution reaction of wollastonite in NaCl-H_2O solutions at high T and P is

$$\underset{\text{wollastonite}}{CaSiO_3} + NaCl + 2\ H_2O = CaCl^+ + OH^- + NaH_3SiO_4 \quad (1)$$

Equation 1 indicates that wollastonite reacts with NaCl and H_2O in proportions of 1:2 to produce three main solute species, each of which has the concentration of m_{CS} (within measurement uncertainties). Evidence for a NaCl/H_2O ratio of 1:2 is the observed maximum in the variation with X_{NaCl} of relative solubility, X_{CS}/X°_{CS}, at X_{NaCl} = 0.30–0.45, where X_{CS} and X°_{CS} are mole fractions of $CaSiO_3$ at the X_{NaCl} of interest and initially pure H_2O, respectively, at the same P and T. A maximum in accord with the stoichiometric coefficients of reaction 1 would be at X_{NaCl} = 0.33. The other requirements of reaction 1 are generation of high pH, as suggested by basic quench fluids, and the necessity of overall charge balance. The neutral complex NaH_3SiO_4 was suggested by Anderson and Burnham (1967) to explain enhancement of quartz solubility in NaCl solutions at low pressure. Quartz solubility enhancement in pH-neutral NaCl solutions does not occur at 10 kbar (Newton and Manning 2000), but it can be shown that the complex would be greatly favored in silica-rich solutions by high pH, even at elevated pressures. Sodium-bearing quench roe in similar experiments on corundum (Newton and Manning 2008) support the Na-silicate complex. The NaCl:H_2O ratio of 1:2 in Equation 1 means that, to a first approximation, the activity of solute $CaSiO_{3,aq}$, a_{CS}, should be proportional to the cube of X_{CS}.

The dissolution model of Equation 1 can be tested by comparing the Gibbs free energy of the reaction:

$$\underset{\text{wollastonite}}{3CaSiO_3} + \underset{\text{hematite}}{Fe_2O_3} = \underset{\text{andradite}}{Ca_3Fe_2Si_3O_{12}} \quad (2)$$

at 800 °C, 10 kbar, calculated in two ways: first, by derivation from the solubility results of the present work and of Newton and Manning (2006); and second, from values taken from internally consistent thermodynamic data sets, which are in close agreement

(±3 kJ/mol, Table 4). The dissolution equilibrium for andradite in the presence of hematite (point 1, Fig. 4) can be written as

$$\underset{\text{andradite}}{Ca_3Fe_2Si_3O_{12}} = \underset{\text{hematite}}{Fe_2O_3} + 3\ CaSiO_{3,aq} \quad (3)$$

Assuming that the very small amount of Fe_2O_3 in solution does not materially influence the solubility of wollastonite, equilibrium among andradite, wollastonite and fluid (point 2, Fig. 4) can be written as

$$3\ \underset{\text{wollastonite}}{CaSiO_3} = 3\ CaSiO_{3,aq} \quad (4)$$

Subtracting Equilibrium 4 from Equilibrium 3 gives:

$$\Delta_r G_2 = 3RT \ln\left(\frac{a_{CS,1}}{a_{CS,2}}\right) \quad (5)$$

where $\Delta_r G_2$ is the Gibbs free energy change of reaction 2, and $a_{CS,1}$ and $a_{CS,2}$ denote activity of $CaSiO_{3,aq}$ at invariant points 1 and 2, respectively (Fig. 4). The activities can be related to concentrations by assuming that activity coefficients cancel over the relatively small difference in $CaSiO_{3,aq}$ molality between points 1 and 2. If wollastonite dissolution yields three solute species according to Equation 1 (Newton and Manning 2006), then $a_{CS,i} = m^3_{CS,i}$, giving

$$\Delta_r G_2 = 3RT \ln\left(\frac{m_{CS,1}}{m_{CS,2}}\right)^3 \quad (6)$$

which can be solved using $m_{CS,1} = 0.0838$ (reagent hematite, Fig. 3), and $m_{CS,2} = 0.1253$ (Newton and Manning 2006) to give $\Delta_r G_2 = -32.31 \pm 2.45$ kJ. This value agrees well with independently determined values (Table 4). If the results for the natural hematite are used, the value would be $\Delta_r G_2 = -27.02 \pm 1.45$ kJ. This value is ~3 kJ less negative than others in Table 4.

The agreement between $\Delta_r G_2$ calculated from solubility data and published sources indicates that the model for the solute state of $CaSiO_{3,aq}$ in NaCl solutions at high T and P given in Equation 1 may be valid. Subject to the adopted assumptions, any reaction involving three solute species would give the same result; however, reactions involving, for example, four or two species would yield values for $\Delta_r G_2$ that are 11 kJ more or less negative than the value obtained using three species—clearly at odds with the independently determined value. Additional, minor dissociation products are probably present, but their abundance must be too low to determine using this approach.

TABLE 4. Summary of ΔG_r of reaction 2 from various sources

ΔG_r (kJ/mol)	Source
–32.07	Kelsey et al. (2004)
–30.01	Gottschalk (1997)
–29.84	Berman and Aranovich (1996)
–32.08	Holland and Powell (1998)
–30.99	Helgeson et al. (1978)
–32.21	This study (reagent hematite)

GEOLOGICAL APPLICATIONS

The present solubility measurements show that andradite is incongruently soluble in H_2O-NaCl solutions at high P, T, and elevated f_{O_2}. The $CaSiO_3$ component is much more soluble than the Fe_2O_3 component. This result contrasts with experiments at lower T and P on the solubility of magnetite (Chou and Eugster 1977) and of Fe in model pelite systems (Althaus and Johannes 1969), where Fe solubility is quite substantial. Both studies were performed at high f_{O_2} (hematite present) in moderately concentrated chloride solutions. In the latter study, carried out at 1000 bars, Fe is, after K and Na, the most soluble cationic component at the highest temperature and salinity investigated (550 °C and 2 *m* NaCl) and is much more soluble than Ca. The main difference between these experiments and the present ones, apart from the *P-T* conditions, is that the earlier experiments were done in acid solutions. The calculated pH of Chou and Eugster (1977) varied from 0 to 2, whereas the estimated pH of the Althaus and Johannes (1969) experiments was 1–2. In the present experiments, the quench pH is quite basic (11–12), which though qualititative, suggests neutral to alkaline conditions at high P and T (Newton and Manning 2008). The low solubility of Fe compared to Ca likely results, at least in part, from the high pH.

These considerations bear on the contrasting geochemical behavior in skarns and in high-grade calc-silicate parageneses. In skarns, a high flux of externally derived acidic, chloride-bearing solutions (e.g., Roedder 1971; Kilinc and Burnham 1972; Webster et al. 1999) leads to elevated Fe solubility and mobility; however, high-grade, andradite-bearing parageneses suggest that fluids must have been small in amount and essentially rock-buffered (Dasgupta and Pal 2005) or perhaps virtually absent and insignificant (Buick et al. 1993). This inference is based on small, local (centimeter scale) variations of mineral associations and compositions that apparently require correspondingly small-scale variations in the activities of CO_2, H_2O, and O_2. The volatile-component activities calculated for the parageneses usually are based on a C-O-H fluid. Previous studies have not considered concentrated NaCl solutions; such fluids could account for both the low H_2O activity, which is generally required for granulite-facies metamorphism, and CO_2 activities ranging from high (required for some scapolite-grandite parageneses, Moecher and Essene 1991; Baker and Newton 1995; Dasgupta and Pal 2005) to moderate or low (required for clinozoisite-grandite associations, Moecher and Essene 1991). Our experiments place constraints on the role of a NaCl-H_2O solution on grandite formation.

Grandite-bearing calc-silicate boudins enclosed by metapelites at a locality in East Antarctica were described by Buick et al. (1993). The Mid-Proterozoic granulite-facies metamorphism at 840 ± 40 °C and 7–9 kbar created zoned calc-silicate pods a few tens of centimeters across. The Ca-rich cores contain the assemblage grandite-scapolite-wollastonite-calcite-quartz. In outer zones, the scapolite and calcite are lost and the garnet becomes progressively poorer in andradite and grossular components. Calcium in the bulk rock decreases markedly from core to outer zones, and silica increases substantially. Iron, however, remains essentially constant from core to outer zones. The contrasting mobilities shown by the Ca and Fe zonation would be compatible with the presence of a small amount of NaCl-rich pore solution,

buffered at high pH by the high Ca content of the boudins, as a metasomatic agent, as shown by the present experiments. It has not yet been demonstrated that a nearly NaCl-free carbonate scapolite can coexist with a concentrated NaCl solution at high *P* and *T*, however.

More generally, where metasomatic alteration has affected calc-silicate gneisses at high metamorphic grade, it is important to know which oxides are most likely to be immobile during this process. The present results suggest that, where H_2O-NaCl solutions are responsible for metasomatism, Fe_2O_3 is significantly less soluble than Al_2O_3 and, all else being equal, is therefore more likely to be conserved in the rock during alteration.

Acknowledgments

This research was supported by U.S. National Science Foundation grant EAR-0337170 (CEM). The work was conducted while J.L.W. was visiting UCLA on graduate exchange from the Australian National University. J.L.W. acknowledges the generous support provided by an ANU MPhil scholarship. We thank J.G. Liou and C. Schmidt for insightful reviews of the manuscript.

References cited

Althaus, E. and Johannes, W. (1969) Experimental metamorphism of NaCl-bearing aqueous solutions by reaction with silicates. American Journal of Science, 267, 87–98.

Anderson, G.M. and Burnham, C.W. (1967) Reactions of quartz and corundum with aqueous chloride and hydroxide solutions at high temperatures and pressures. American Journal of Science, 265, 12–27.

Baker, J. and Newton, R.C. (1995) Experimentally determined activity-composition relations for Ca-rich scapolite in the system $CaAl_2Si_2O_8$-$NaAlSi_3O_8$-$CaCO_3$ at 7 kbar. American Mineralogist, 80, 744–751.

Berman, R.G. and Aranovich, L.Y. (1996) Optimized standard state and solution properties of minerals. 1. Model calibration for olivine, orthopyroxene, cordierite, garnet, ilmenite in the system FeO-MgO-CaO-Al_2O_3-TiO_2-SiO_2. Contributions to Mineralogy and Petrology, 124, 1–24.

Boctor, N.Z., Popp, R.K., and Frantz, J.D. (1980). Mineral-solution equilibria—IV. Solubilities and the thermodynamic properties of $FeCl^0_2$ in the system Fe_2O_3-H_2-H_2O-HCl. Geochimica et Cosmochimica Acta, 44, 1509–1518.

Buick, I.S., Harley, S.L., and Cartwright, I.C. (1993) Granulite facies metasomatism: Zoned calc-silicate boudins from the Rauer Group, East Antarctica. Contributions to Mineralogy and Petrology, 113, 557–571.

Burt, D.M. (1972) The facies of some Ca-Fe-Si skarns in Japan. Proceedings of the 24th International Geological Congress, Section 2, 284–288.

Caciagli, N.C. and Manning, C.E. (2003) The solubility of calcite in water at 5–16 kbar and 500 to 800 °C. Contributions to Mineralogy and Petrology, 42, 275–285.

Carmichael, D.M. (1969) On the mechanism of prograde metamorphic reactions in quartz-bearing pelitic rocks. Contributions to Mineralogy and Petrology, 20, 244–267.

Chou, I.-M. and Eugster, H.P. (1977) Solubility of magnetite in supercritical chloride solutions. American Journal of Science, 277, 1296–1314.

Dasgupta, S. and Pal, S. (2005) Origin of grandite garnet in calc-silicate granulites: mineral-fluid equilibria and petrogenetic grids. Journal of Petrology, 46, 1045–1076.

Einaudi, M.T., Meinert, L.D., and Newberry, R.J. (1981) Skarn deposits. Economic Geology, Seventy-Fifth Anniversary Volume, 317–391.

Fockenberg, T., Burchard, M., and Maresch, W.V. (2004) Solubilities of calcium silicates at high pressures and temperatures. Lithos, 73, S37.

Gottschalk, M. (1997) Internally consistent thermodynamic data for rock-forming minerals in the system SiO_2-TiO_2-Al_2O_3-Fe_2O_3-CaO-MgO-FeO-H_2O-Na_2O-H_2O-CO_2. European Journal of Mineralogy, 9, 175–223.

Gustafson, W.I. (1974) The stability of andradite, hedenbergite and related minerals in the system Ca-Fe-O-H. Journal of Petrology, 15, 455–496.

Helgeson, H.C., Delany, J.M., Nesbitt, H.W., and Bird, D.K. (1978) Summary and critique of the thermodynamic properties of rock-forming minerals. American Journal of Science, 278A, 1–204.

Holland, T.J.B. and Powell, R. (1998) An internally consistent data set for phases of petrologic interest. Journal of Metamorphic Geology, 16, 309–343.

Huckenholz, H.G. (1969) Synthesis and stability of Ti-andradite. American Journal of Science, 267-A, 209–232.

Huckenholz, H.G. and Knittel, D. (1976) Uvarovite: Stability of uvarovite-andradite solid solutions at low pressure. Contributions to Mineralogy and Petrology, 56, 61–76.

Huckenholz, H.G. and Yoder, H.S., Jr. (1971) Andradite stability relations in the $CaSiO_3$-Fe_2O_3 join up to 30 kb. Neues Jahrbuch für Mineralogie Abhandlungen, 114, 246–280.

Huckenholz, H.G., Lindhuber, W., and Springer, J. (1974) The join $CaSiO_3$-Al_2O_3-Fe_2O_3 of the CaO-Al_2O_3-Fe_2O_3-SiO_2 quaternary system and its bearing on the formation of grandite garnets and fassaitic pyroxenes. Neues Jahrbuch für Mineralogie, Abhandlungen, 121, 160–207.

Kelsey, D.E., White, R.W., Holland, T.J.B., and Powell, R. (2004) Calculated phase equilibria in K_2O-FeO-MgO-Al_2O_3-SiO_2 for sapphirine-quartz-bearing mineral assemblages. Journal of Metamorphic Geology, 22, 559–578.

Kilinc, I.A. and Burnham, C.W. (1972) Partitioning of chloride between a silicate melt and coexisting aqueous phase from 2 to 8 kbar. Economic Geology, 67, 231–235.

Liou, J.G. (1974) Stability relations of andradite-quartz in the system Ca-Fe-Si-O-H. American Mineralogist, 59, 1016–1025.

Manning, C.E. (2007) Solubility of corundum + kyanite in H_2O solutions at 700 °C and 10 kbar: evidence for Al-Si complexing at high pressure and temperature. Geofluids, 7, 258–269.

Moecher, D.P. and Chou, I.-M. (1990) Experimental investigation of andradite and hedenbergite equilibria. American Mineralogist, 75, 1327–1341

Moecher, D.P. and Essene, E.J. (1991) Calculation of CO_2 activity using scapolite equilibria: Constraints on the presence and composition of a fluid phase during high grade metamorphism. Contributions to Mineralogy and Petrology, 108, 219–240.

Newton, R.C. and Manning, C.E. (2000) Quartz solubility in H_2O-NaCl and H_2O-CO_2 solutions at deep crust-upper mantle pressures and temperatures: 2–15 kbar and 500–900 °C. Geochimica et Cosmochimica Acta, 64, 2993–3005.

——— (2006) Solubilities of corundum, wollastonite and quartz in H_2O-NaCl solutions at 800 °C and 10 kbar: Interaction of simple minerals with brines at high pressure and temperature. Geochimica et Cosmochimica Acta, 70, 5571–5582.

——— (2007) Solubility and stability of grossular, $Ca_3Al_2Si_3O_{12}$, in the system CaO-Al_2O_3-NaCl-H_2O at 800 °C and 10 kbar. Geochimica et Cosmochimica Acta, in press.

——— (2008) Solubility of corundum in the system Al_2O_3-SiO_2-H_2O-NaCl at 800 °C and 10 kbar. Chemical Geology, in press.

Roedder, E. (1971) Fluid inclusion studies on porphyry-type ore deposits at Bingham, Utah, Butte, Montana, and Climax, Colorado. Economic Geology, 46, 98–120.

Sengupta, P. and Raith, M.M. (2002) Garnet composition as a petrogenetic indicator: An example from a marble-calc-silicate granulite interface at Kondapalle, Eastern Ghats Belt, India. American Journal of Science, 302, 686–725.

Sengupta, P., Sanyal, S., Dasgupta, S., Fukuoka, M., Ehl, J., and Pal, S. (1997) Controls of mineral reactions in high-grade garnet-wollastonite-scapolite-bearing calc-silicate rocks: An example from Anakapalle, Eastern Ghats, India. Journal of Metamorphic Geology, 15, 551–564.

Simon, A.C., Pettke, T., Candela, P.A., Piccoli, P.M., and Heinrich, C.A. (2004) Magnetite solubility and iron transport in magmatic-hydrothermal environments. Geochimica et Cosmochimica Acta, 68, 4905–4914.

Suwa, Y., Tamai, Y., and Naka, S. (1976) Stability of synthetic andradite at atmospheric pressure. American Mineralogist, 61, 26–28.

Taylor, B. and Liou, J.G. (1978) The low temperature stability of andradite in C-O-H fluids. American Mineralogist, 63, 378–393

Tropper, P. and Manning, C.E. (2007) The solubility of corundum in H_2O at high pressure and temperature and its implications for Al mobility in the deep crust and upper mantle. Chemical Geology, 240, 54–60.

Webster, J.D., Kinzler, R.J., and Mathez, E.A. (1999) Chloride and water solubility in basalt and andesite liquids and implications for magmatic degassing. Geochimica et Cosmochimica Acta, 63, 729–738.

Whitney, J.A., Hemley, J.J., and Simon, F.O. (1985). The concentration of iron in chloride solutions equilibrated with synthetic granitic compositions: The sulfur-free system. Economic Geology, 80, 444–460.

Zhang, Z. and Saxena, S.K. (1991) Thermodynamic properties of andradite and applications to skarn with coexisting andradite and hedenbergite. Contributions to Mineralogy and Petrology, 107, 255–263.

Manuscript received July 9, 2007
Manuscript accepted December 21, 2007
Manuscript handled by Matthias Gottschalk